CONF-850506--5

Statistical Fluctuations in Heavy-Charged-Particle Tracks[1]

R. N. Hamm, J. E. Turner, and H. A. Wright

CONF-850506--5

DE85 012100

Health and Safety Research Division
Oak Ridge National Laboratory
Oak Ridge, Tennessee

Statistical Fluctuation

FOOTNOTES

[1]Research sponsored jointly by the Solid State Sciences Division, Rome Air Development Center, under Interagency Agreement DOE No. 40-226-70 and the Office of Health and Environmental Research, U.S. Department of Energy, under contract DE-AC05-840R21400 with Martin Marietta Energy Systems, Inc.

Statistical Fluctuations in Heavy-Charged-Particle Tracks

R. N. Hamm, J. E. Turner, and H. A. Wright

ABSTRACT

We present the results of the following Monte Carlo track-segment calculations for protons with energies of 1, 2, 5, and 10 MeV in liquid water: (1) radial dose around a long segment of a proton track; (2) energy-loss straggling distributions for protons of different energies in 1 μm of water; (3) the distribution in the average absorbed dose around track segments of various lengths; (4) the relative standard deviations in these distributions as functions of the length of the track segments. Calculations such as those presented here are useful for studying track phenomena on a microdosimetric scale, where statistical fluctuations are substantial.

INTRODUCTION

The chemical and biological effects of radiation are frequently interpreted in terms of average track-segment quantities, such as LET and radial dose, pertaining to heavy charged particles. These quantities reflect only indirectly the statistical fluctuations in particle transport that are the subject of microdosimetry. In many instances, particularly when one deals with relatively short track segments ($\lesssim$1 μm in H_2O), these fluctuations can have an all-important influence in producing chemical and subsequent biological changes. In this paper, we present the results of Monte Carlo calculations of track segments of protons with energies of 1, 2, 5, and 10 MeV in liquid water. The computations were performed with the computer code OREC,[1] which treats in detail the histories of all secondary electrons until their energies go below the threshold, 7.4 eV, for producing electronic transitions.

RADIAL DOSE

Figure 1 shows the average doses around the tracks of a 1-MeV proton and a 10-MeV proton as functions of the radial distance from the proton's trajectory. The doses are averaged in radial bins in the intervals shown by the histograms. The results were calculated from very long track segments generated by protons moving at constant velocity. The calculations are compared with measurements [2] (shown on the figure as a continuous curve) for 1-MeV protons in tissue-equivalent gas normalized to unit density. The curves show the well recognized behavior of radial dose, which rapidly drops many orders of magnitude with distance from the track. The dose for the 1-MeV proton, which has the higher LET, is larger in the immediate vicinity of the track.

However, the faster, 10-MeV proton can produce delta rays with higher energies than those from the 1-MeV proton; so its radial-dose curve is higher at large distances from the track.

Radial dose, averaged in the manner just described, is an abstraction that is not characteristic of single proton track segments because of fluctuation phenomena. Figure 2 shows an end-on "picture" of two different lengths from the same segment of a calculated track of a 1-MeV proton. Each dot represents the location of an inelastic event, resulting in the creation of an ionized or excited species, H_2O^+ or H_2O^*, produced directly by the incident proton or a secondary electron. While the figure does not display radial dose, there is a high correlation between the density of dots and the radial dose averaged along the portion of the track that is represented. Even for the longer, 1000-nm segment, one sees that the absorbed dose is not symmetric about the track. The type of distributions shown in Fig. 1 are not realized by individual particles in such segment lengths. The importance of fluctuations becomes more pronounced on a smaller scale, as seen in the view of the 100-nm segment shown in the lower portion of Fig. 2.

ENERGY STRAGGLING

Statistical fluctuations in energy loss are responsible for the phenomenon of energy straggling – the unequal energy losses experienced by particles that travel the same distance under identical conditions. The calculated distributions of energy loss for protons of several energies, traversing 1 μm of liquid water, are shown in Fig. 3. The vertical arrows at each proton energy mark the average energy loss, which, since we are dealing with 1-μm segments, is numerically equal to

the stopping power dE/dx in keV/μm. At the lowest LET (10-MeV protons), the average number of collisions in 1 μm is smallest. The skewed distribution for this energy reflects both this fact and the existence of the high-energy-loss tail that characterizes the proton-electron single-collision spectrum. (The maximum energy that a 10-MeV proton can lose in a single collision with an electron, initially free and at rest, is 21.9 keV.) The curve for 10 MeV in Fig. 3 shows that the most probable value of the energy loss is about one-half the value implied by the stopping power. The shape of the curve in this peak region is approximately Gaussian, reflecting a large number of small energy-loss collisions. The high-energy losses are rare, but they contribute about one-half of dE/dx, which is the first moment of the single-collision energy-loss spectrum. Figure 3 illustrates clearly that estimates of dose based on 1-μm track-segment averages for 10-MeV protons could be misleading.

For successively lower proton energies, the LET and average energy loss in a 1-μm segment increase, as the other curves in Fig. 3 illustrate. The larger number of collisions in the segment tends to suppress the skewing of the high-loss spectrum. The curves become progressively more Gaussian in shape, and the most probable energy loss gets closer to that predicted from the stopping power. At 1 MeV, the distribution of energy losses has an appearance consistent with that expected from "long-pathlength," or Gaussian, energy-straggling theory.

DOSE DISTRIBUTION IN TRACK SEGMENTS OF DIFFERENT LENGTHS

As distinct from the distribution in energy loss along an ion track, we have also calculated the distribution in energy deposited (proportional to the total dose) around segments of different lengths.

The energy-loss and energy-absorbed distributions are the same for long track segments, but are considerably different over short segments. Some results are shown in Fig. 4 for 1-MeV protons. The longest segment, 1000 nm, has the same length as that used in calculating the 1-MeV curve in Fig. 3. It is seen that the two distributions are similar. However, the dose distributions for shorter segments are considerably different. The most probable value of the dose decreases steadily as the segment length gets shorter. At the same time, the probability of finding relatively large doses increases. (The average dose is independent of the segment length and is proportional to the stopping power.) On the smallest scale considered, many randomly selected 1-nm segments occur in which the dose is zero. For clarity, the lower-energy portion of this curve is shown as a histogram. No primary or secondary interactions take place in these segments of the track. As seen from Fig. 4, the most probable value of the dose in a 1-nm segment is zero.

FLUCTUATIONS IN DOSE IN SEGMENTS OF DIFFERENT LENGTHS

We have studied the fluctuations of dose in track segments as a function of the segment length for 1-, 2-, 5-, and 10-MeV protons. The results are shown in Fig. 5 in terms of the relative error, or ratio of the standard deviation, σ, and mean energy deposited, ΔE. The relative error for a given length is greater for particles with smaller stopping power. (Based on Poisson statistics, $\sigma/\Delta E$ varies as the inverse square root of the number of inelastic events, which, in turn, is proportional to the stopping power.) The curves in Fig. 5 show quantitatively how widely the dose around track segments of a given length can fluctuate. They can also be used to determine how long a segment must be in order that the average fluctuation in dose be less than a given value.

SUMMARY

The calculations presented here have focused primarily on statistical fluctuations that occur along the tracks of protons in liquid water. Examples show that fluctuations on a microdosimetric scale produce events that can be quite different from those predicted from track-average quantities, such as radial dose and stopping power.

REFERENCES

1. Hamm, R. N., Turner, J. E., Ritchie, R. H., and Wright, H. A. Calculation of Heavy-Ion Tracks in Liquid Water. Radiat. Res. (submitted).

2. Wingate, C. L. and Baum, J. W. Measured Radial Distributions of Dose and LET for Alpha and Proton Beams in Hydrogen and Tissue-Equivalent Gas. Radiat. Res. 65, 1-19 (1976).

FIGURE CAPTIONS

Fig. 1. Average dose as a function of radial distance from track segments of 1-MeV and 10-MeV protons in liquid water. The histograms give the results of the present calculations. The continuous curve shows the measurements of Wingate and Baum[2] for 1-MeV protons in tissue-equivalent gas normalized to unit density.

Fig. 2. End-on view of 1000-μm and 100-μm portions from the same track segment of a 1-MeV proton in liquid water.

Fig. 3. Spectrum of energy losses in keV calculated for 1-, 2-, 5-, and 10-MeV protons traversing 1 μm of liquid water. Vertical arrows mark the stopping power at each energy in keV/μm.

Fig. 4. Probability distributions for deposition of different amounts of energy (in eV/nm) along 1000-, 100-, 10-, and 1-nm segments of tracks of 1-MeV protons in liquid water.

Fig. 5. Relative error, or ratio of standard deviation σ and mean energy deposited ΔE, as a function of length of track segment for protons of energy 1, 2, 5, and 10 MeV.

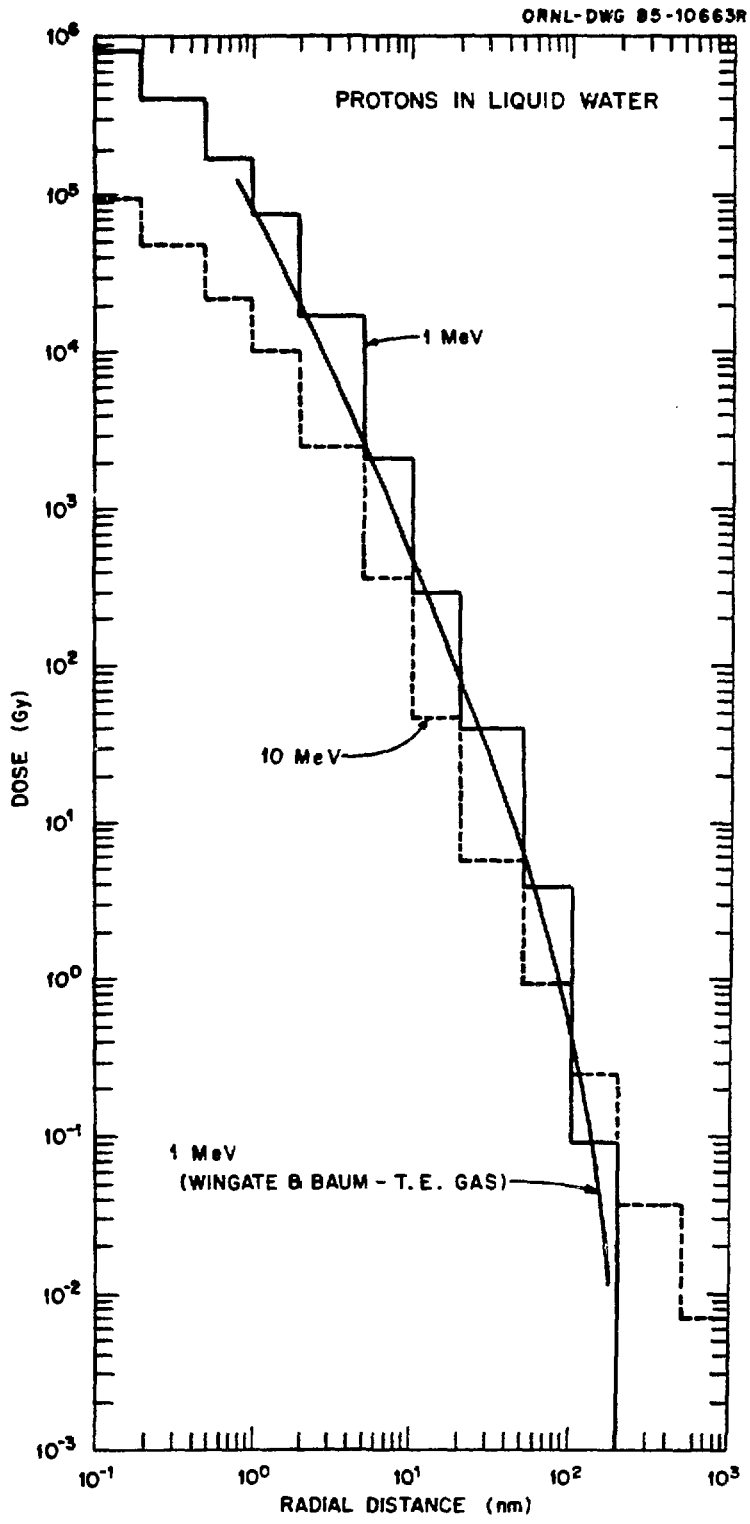
ORNL-DWG 85-10663R
PROTONS IN LIQUID WATER
1 MeV
10 MeV
1 MeV
(WINGATE & BAUM - T.E. GAS)
DOSE (Gy)
RADIAL DISTANCE (nm)
10^6
10^5
10^4
10^3
10^2
10^1
10^0
10^-1
10^-2
10^-3
10^-1
10^0
10^1
10^2
10^3

Fig. 1

ORNL-DWG 85-10666

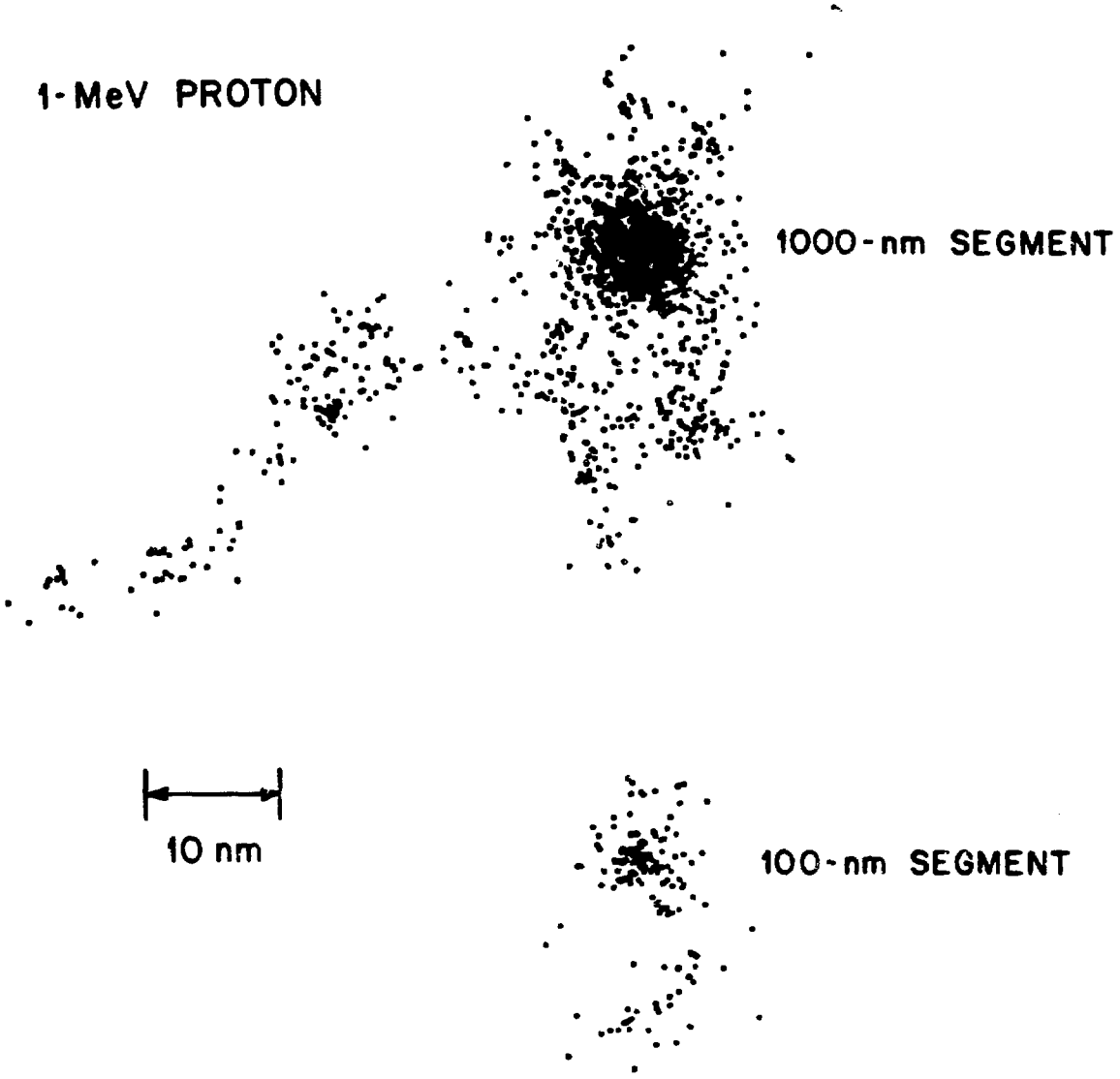

Fig. 2

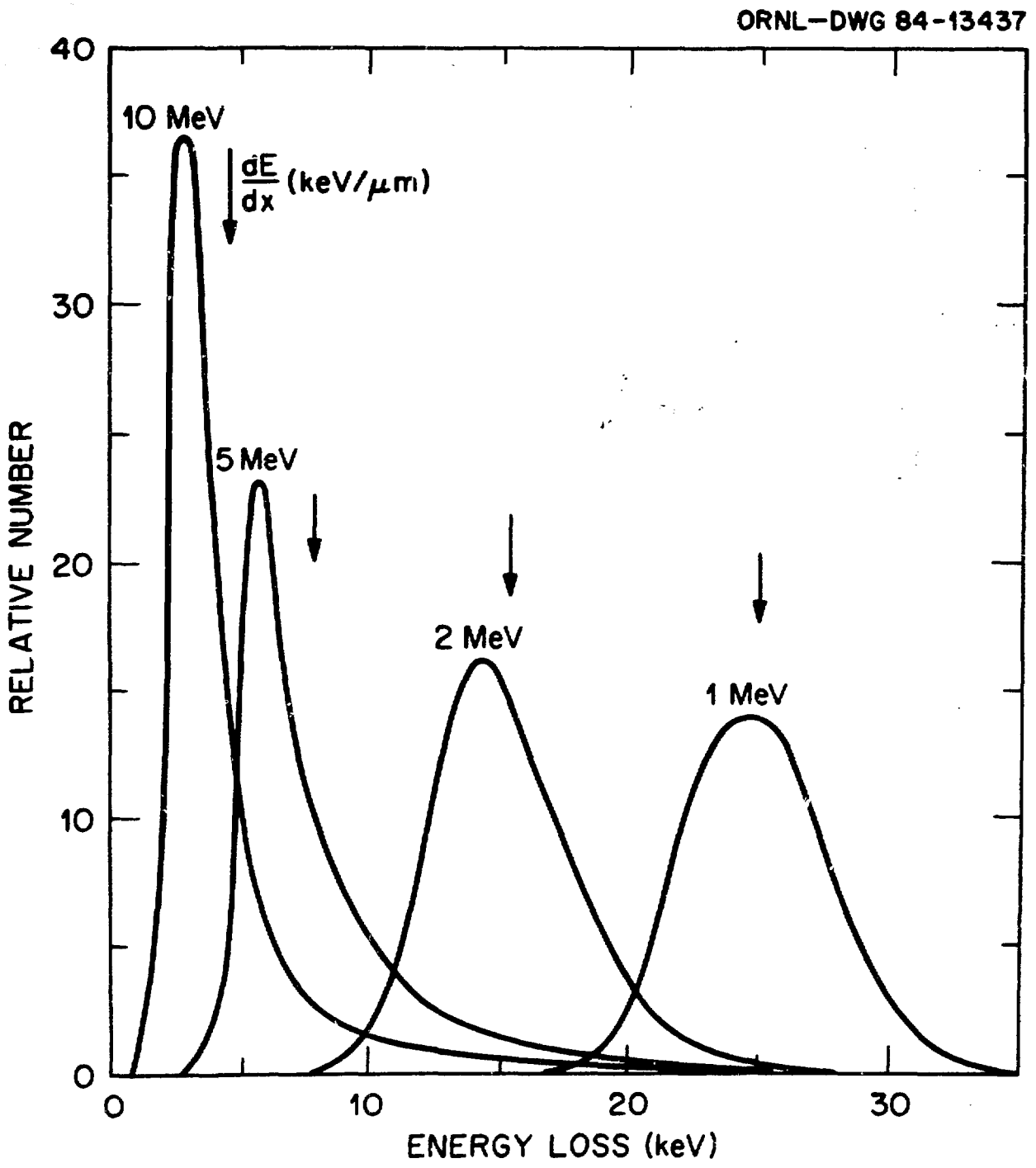
ORNL-DWG 84-13437
40
30
20
10
0
RELATIVE NUMBER
10 MeV
dE/dx (keV/μm)
5 MeV
2 MeV
1 MeV
0
10
20
30
ENERGY LOSS (keV)

Fig. 3

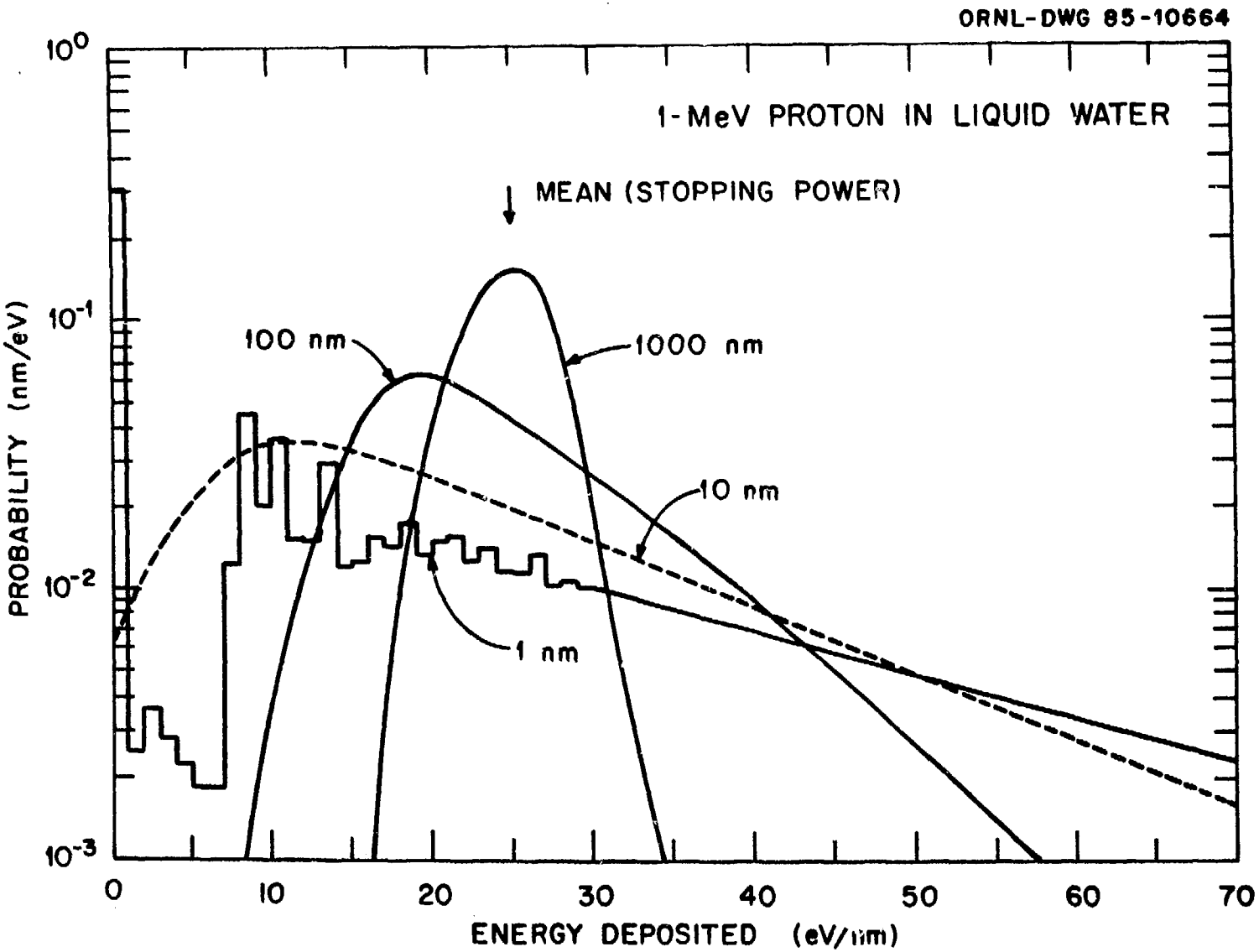
ORNL-DWG 85-10664
1-MeV PROTON IN LIQUID WATER
MEAN (STOPPING POWER)
100 nm
1000 nm
10 nm
1 nm
PROBABILITY (nm/eV)
ENERGY DEPOSITED (eV/nm)
10^0
10^{-1}
10^{-2}
10^{-3}
0
10
20
30
40
50
60
70

Fig. 4

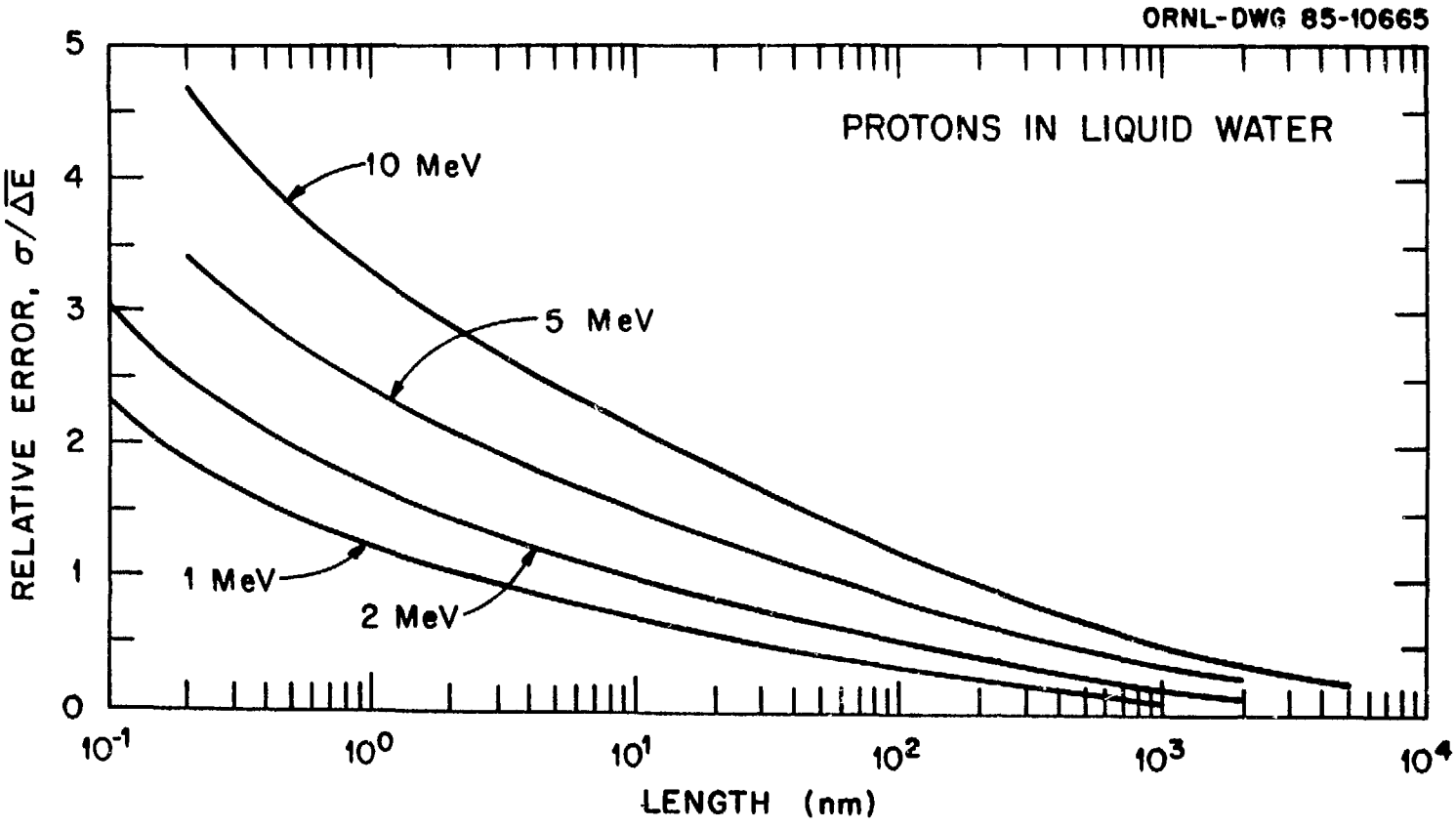
ORNL-DWG 85-10665
PROTONS IN LIQUID WATER
10 MeV
5 MeV
2 MeV
1 MeV
RELATIVE ERROR, σ/ΔE
LENGTH (nm)
0
1
2
3
4
5
10^-1
10^0
10^1
10^2
10^3
10^4

Fig. 5